

Swine Influenza H1N1 Virus Induces Acute Inflammatory Immune Responses in Pig Lungs: a Potential Animal Model for Human H1N1 Influenza Virus[∇]

Mahesh Khatri,¹ Varun Dwivedi,¹ Steven Krakowka,² Cordelia Manickam,¹ Ahmed Ali,¹ Leyi Wang,¹ Zhuoming Qin,^{1,3} Gourapura J. Renukaradhya,^{1,4*} and Chang-Won Lee^{1,4*}

Food Animal Health Research Program, Ohio Agricultural Research and Development Center, the Ohio State University, 1680 Madison Avenue, Wooster, Ohio 44691¹; Department of Veterinary Biosciences, College of Veterinary Medicine, the Ohio State University, Columbus, Ohio 43210²; Institute of Poultry Science, Shandong Academy of Agricultural Sciences, Jinan, People's Republic of China 250023³; and Department of Veterinary Preventive Medicine, College of Veterinary Medicine, the Ohio State University, Columbus, Ohio 43210⁴

Received 5 June 2010/Accepted 10 August 2010

Pigs are capable of generating reassortant influenza viruses of pandemic potential, as both the avian and mammalian influenza viruses can infect pig epithelial cells in the respiratory tract. The source of the current influenza pandemic is H1N1 influenza A virus, possibly of swine origin. This study was conducted to understand better the pathogenesis of H1N1 influenza virus and associated host mucosal immune responses during acute infection in humans. Therefore, we chose a H1N1 swine influenza virus, Sw/OH/24366/07 (SwIV), which has a history of transmission to humans. Clinically, inoculated pigs had nasal discharge and fever and shed virus through nasal secretions. Like pandemic H1N1, SwIV also replicated extensively in both the upper and lower respiratory tracts, and lung lesions were typical of H1N1 infection. We detected innate, proinflammatory, Th1, Th2, and Th3 cytokines, as well as SwIV-specific IgA antibody in lungs of the virus-inoculated pigs. Production of IFN- γ by lymphocytes of the tracheobronchial lymph nodes was also detected. Higher frequencies of cytotoxic T lymphocytes, $\gamma\delta$ T cells, dendritic cells, activated T cells, and CD4⁺ and CD8⁺ T cells were detected in SwIV-infected pig lungs. Concomitantly, higher frequencies of the immunosuppressive T regulatory cells were also detected in the virus-infected pig lungs. The findings of this study have relevance to pathogenesis of the pandemic H1N1 influenza virus in humans; thus, pigs may serve as a useful animal model to design and test effective mucosal vaccines and therapeutics against influenza virus.

Swine influenza is a highly contagious, acute respiratory viral disease of swine. The causative agent, swine influenza virus (SwIV), is a strain of influenza virus A in the *Orthomyxoviridae* family. Clinical disease in pigs is characterized by sudden onset of anorexia, weight loss, dyspnea, pyrexia, cough, fever, and nasal discharge (21). Porcine respiratory tract epithelial cells express sialic acid receptors utilized by both avian (α -2,3 SA-galactose) and mammalian (α -2,6 SA-galactose) influenza viruses. Thus, pigs can serve as “mixing vessels” for the generation of new reassortant strains of influenza A virus that may contain RNA elements of both mammalian and avian viruses. These “newly generated” and reassorted viruses may have the potential to cause pandemics in humans and enzootics in animals (52).

Occasional transmission of SwIV to humans has been reported (34, 43, 52), and a few of these cases resulted in human deaths. In April 2009, a previously undescribed H1N1 influenza virus was isolated from humans in Mexico. This virus has spread efficiently among humans and resulted in the current

human influenza pandemic. Pandemic H1N1 virus is a triple reassortant (TR) virus of swine origin that contains gene segments from swine, human, and avian influenza viruses. Considering the pandemic potential of swine H1N1 viruses, it is important to understand the pathogenesis and mucosal immune responses of these viruses in their natural host. Swine can serve as an excellent animal model for the influenza virus pathogenesis studies. The clinical manifestations and pathogenesis of influenza in pigs closely resemble those observed in humans. Like humans, pigs are also outbred species, and they are physiologically, anatomically, and immunologically similar to humans (9, 23, 39, 40). In contrast to the mouse lung, the porcine lung has marked similarities to its human counterpart in terms of its tracheobronchial tree structure, lung physiology, airway morphology, abundance of airway submucosal glands, and patterns of glycoprotein synthesis (8, 10, 17). Furthermore, the cytokine responses in bronchoalveolar lavage (BAL) fluid from SwIV-infected pigs are also identical to those observed for nasal lavage fluids of experimentally infected humans (20). These observations support the idea that the pig can serve as an excellent animal model to study the pathogenesis of influenza virus.

Swine influenza virus causes an acute respiratory tract infection. Virus replicates extensively in epithelial cells of the bronchi and alveoli for 5 to 6 days followed by clearance of viremia by 1 week postinfection (48). During the acute phase of the

* Corresponding author. Mailing address: Food Animal Health Research Program, Ohio Agricultural Research and Development Center, the Ohio State University, 1680 Madison Avenue, Wooster, OH 44691. Phone for G. J. Renukaradhya: (330) 263-3748. Fax: (330) 263-3677. E-mail: gourapura.1@osu.edu. Phone for C.-W. Lee: (330) 263-3750. Fax: (330) 263-3677. E-mail: lee.2854@osu.edu.

[∇] Published ahead of print on 18 August 2010.

disease, cytokines such as alpha interferon (IFN- α), tumor necrosis factor alpha (TNF- α), interleukin-1 (IL-1), IL-6, IL-12, and gamma interferon (IFN- γ) are produced. These immune responses mediate both the clinical signs and pulmonary lesions (2). In acute SwIV-infected pigs, a positive correlation between cytokines in BAL fluid, lung viral titers, inflammatory cell infiltrates, and clinical signs has been detected (2, 48).

Infection of pigs with SwIV of one subtype may confer complete protection from subsequent infections by homologous viruses and also partial protection against heterologous subtypes, but the nature of the immune responses generated in the swine are not fully delineated. Importantly, knowledge related to host mucosal immune responses in the SwIV-infected pigs is limited. So far only the protective virus-specific IgA and IgG responses in nasal washes and BAL fluid, as well as IgA, IgG, and IgM responses in the sera of infected pigs, have been reported (28). Pigs infected with H3N2 and H1N1 viruses have an increased frequency of neutrophils, NK cells, and CD4 and CD8 T cells in the BAL fluid (21). Pigs infected with the pandemic H1N1 virus showed activated CD4 and CD8 T cells in the peripheral blood on postinfection day (PID) 6 (27). Proliferating lymphocytes in BAL fluid and blood and virus-specific IFN- γ -secreting cells in the tracheobronchial lymph nodes (TBLN) and spleen were detected in SwIV-infected pigs (7). Limited information is available on the mucosal immune responses in pig lungs infected with SwIV, which has a history of transmission to humans.

In this study, we examined the acute infection of SwIV (strain SwIV OH07) in pigs with respect to viral replication, pathology, and innate and adaptive immune responses in the respiratory tract of these pigs. This virus was isolated from pigs which suffered from respiratory disease in Ohio, and the same virus was also transmitted to humans and caused clinical disease (43, 55). Interestingly, like pandemic H1N1 influenza virus, SwIV also infects the lower respiratory tract of pigs. Delineation of detailed mucosal immune responses generated in pig lungs during acute SwIV OH07 infection may provide new insights for the development of therapeutic strategies for better control of virus-induced inflammation and for the design and testing of effective vaccines.

MATERIALS AND METHODS

Virus. Recently isolated TR H1N1 Sw/OH/24366/07 (55) was used to infect pigs. Virus was propagated in Madin-Darby canine kidney (MDCK) cells. The MDCK cells were cultured in Dulbecco's modified Eagle medium (DMEM) supplemented with 10% fetal bovine serum, penicillin-streptomycin, and amphotericin B (Gibco). For the preparation of virus stock and titration, MDCK cells were cultured in DMEM supplemented with TPCK (tolylsulfonyl phenylalanyl chloromethyl ketone)-treated trypsin (1 μ g/ml).

Pigs. As the majority of commercial pigs possess circulating influenza-specific antibodies, we used naturally delivered colostrum-deprived conventional Large White-Duroc crossbred pigs that were raised in our BSL2 facility at the Ohio Agricultural Research and Development Center, the Ohio State University, Wooster, OH. Prior to infection at 2 and 4 to 5 weeks of age, pigs were bled and sera were confirmed negative for the antibodies against H1 and H3 influenza viruses. Pigs were maintained, inoculated, and euthanized in accordance with the standards of the Institutional Laboratory Animal Care and Use Committee, the Ohio State University.

Virus inoculation and management of pigs. Two identical trials were conducted. Pigs were anesthetized using Telazol (Fort Dodge). During each trial, six pigs were inoculated with SwIV OH07 (3.0×10^6 50% tissue culture infective doses [TCID₅₀] [intranasally] and 3.0×10^6 TCID₅₀ [intratracheally]). Six mock-infected pigs inoculated with DMEM were also included in the study. All pigs

were monitored daily for clinical signs of respiratory infection, and rectal temperatures from PID 0 through PID 6 were obtained. Nasal swabs from the virus- and mock-infected pigs were collected daily for virus detection.

Evaluation of gross and histopathologic lesions. Three pigs each from mock- and SwIV-infected group were euthanized on PID 3 and PID 6. At necropsy, the trachea, lung, heart, tonsil, kidney, spleen, liver, TBLN, duodenum, jejunum, ileum, cecum, and colon were examined grossly and a portion (approximately 1 g) of the organ was collected in DMEM for virus isolation and titration. Grossly evident pulmonary changes were assigned a score based upon the percentage of virus-affected lesions (purple-red consolidation, typical of SwIV) in each lung lobe. A total percent involvement for each lung was calculated based on weighted proportions of each lobe to the total lung volume as described previously (19, 24).

For microscopic examination, a small portion of all the above-mentioned organs and the complete right lung were preserved in 10% buffered formalin. The fixed tissues were embedded in paraffin, and 3- μ m sections were cut for histological examination. Examination of tissue sections from this study was conducted by a veterinary pathologist who was blinded to the experimental design and SwIV infection status.

Tissue sections of lungs were stained with hematoxylin and eosin and examined microscopically for bronchiolar epithelial changes and peribronchiolar inflammation as described previously (24, 38). Lesion severity was scored by the distribution or by the extent of lesions within the sections examined, as follows: 0, no visible changes; 1, mild focal or multifocal change, minimally different from the normal; 2, moderate multifocal change; and 3, severe and diffusely distributed change.

Detection of virus replication in tissues. Homogenates (10% [wt/vol]) of individual lung lobes (left cranial, left caudal, right cranial, right middle, right caudal, and accessory lobe), trachea, heart, liver, spleen, kidney, duodenum, ileum, cecum, jejunum, and colon were prepared in DMEM with antibiotics using a tissue homogenizer (Omni homogenizer) (GLH) and Omni Tip plastic generator probes (Omni International). Debris was removed by centrifugation (10 min at $\sim 1,500 \times g$) and the supernatant was collected and filtered through a 0.45- μ m sterile filter. Clarified material was stored at -80°C until being used for the virus titration.

Serial 10-fold dilutions of nasal swab and 10% (wt/vol) homogenate of all the tissues mentioned above were prepared in DMEM supplemented with 1 μ g of TPCK trypsin/ml. MDCK cells cultured in 96-well tissue culture plates were inoculated with the dilutions and were examined for cytopathic effects after 48 to 72 h of incubation at 37°C . Virus titers were calculated by the standard method.

Determination of cytokine concentrations in lung by ELISA. Lung lysates from all the euthanized pigs were prepared as described previously (3, 36) and frozen at -20°C until cytokine analysis by enzyme-linked immunosorbent assay (ELISA). Lung lysates were analyzed for innate (IFN- α), proinflammatory (IL-6), Th2 (IL-4), Th1 (IFN- γ and IL-12), and anti-inflammatory/T-regulatory (IL-10 and transforming growth factor β [TGF- β]) cytokines by ELISA as described previously (1, 24, 36).

ELISA for antigen-specific IgA antibodies. Influenza antigen-specific IgA, IgG, and IgM antibodies were measured by ELISA as described previously (50) with few modifications. Briefly, Maxisorp 96-well plates were coated with a pretitrated concentration (15 μ g/ml) of UV-inactivated SwIV OH07 antigens and incubated overnight at 4°C . The plates were blocked for 2 h at room temperature (RT) with 100 μ l of 1% bovine serum albumin (BSA) in TBST (0.1 M Tris, 0.17 M NaCl, 0.05% Tween 20) and then washed four times with phosphate-buffered saline plus 0.05% Tween 20. Serum and lung lysate samples were added (100 μ l/well) in duplicate, and the plates were incubated for 2 h at RT. Samples of previously defined positive sera and the negative-control sera were run on each plate. Subsequently, the plates were incubated with horseradish peroxidase (HRP)-labeled anti-porcine IgA, IgG, and IgM secondary antibody (KPL) for 2 h. After being washed, the plates were developed using tetramethyl benzidine substrate. The optical density (OD) of the reaction was measured at 450 nm with a microplate reader (Molecular Devices SpectraMax Plus 384). To eliminate the background activity, an influenza antigen-uncoated control plate, blocked and treated exactly as described above, was included side-by-side. The OD values obtained from the experimental plates were subtracted from those of the control plate to obtain corrected OD values.

Isolation of BAL cells, PBMC, tonsils, lung, and TBLN mononuclear cells. Blood was collected in acid citrate dextrose solution. Samples of TBLN and tonsils were collected in DMEM. Isolation of peripheral blood mononuclear cells (PBMC), TBLN mononuclear cells (MNC), and BAL cells was performed using the standard procedures described previously (47). Briefly, tonsils and TBLN were processed through a cell selector (70- μ m tissue screen). Buffy coat cells from peripheral blood were layered on Histopaque (lymphocyte separation me-

dium) (ICN Biomedicals) and centrifuged for 30 min at $400 \times g$. Following Percoll or Histopaque purification, mononuclear cell layers were recovered, erythrocytes were lysed by hypotonic shock using water, and the resulting MNC preparations were washed and resuspended in RPMI medium.

Lung MNC were isolated as described previously (29), with few modifications. Briefly, after euthanasia the pulmonary vasculature was flushed with excess sterile PBS to remove peripheral blood, and lungs were subsequently removed. The airways were lavaged to remove free cells as well as to collect BAL cells as described previously (4) using sterile ice-cold PBS containing EDTA (0.03%). Subsequently, the lung tissue was collected in PBS, washed in sterile PBS, minced and suspended in PBS containing DNase (40 $\mu\text{g}/\text{ml}$) and type II collagenase (1.5 mg/ml), and incubated on an orbital shaker at 37°C for 2 h. Released cells were collected and fractionated using 43 and 70% Percoll density gradient centrifugation, and the interface rich in lung MNC was collected. Cells were counted with a hemacytometer, and viability was tested by trypan blue exclusion and was found to be $>95\%$.

Flow cytometry. Single-cell suspensions were subjected to multicolor immunostaining for flow cytometric analysis. Briefly, cells were resuspended in fluorescence-activated cell sorting (FACS) buffer (Hanks balanced salt solution [HBSS] containing 0.1% BSA and 0.02% sodium azide). Cells were plated in U-bottom 96-well plates and then treated with FACS buffer containing 2% pig serum for 20 min to block Fc receptors. Cells were then stained with either the appropriate monoclonal antibody (MAb) directly conjugated to specific fluorochromes, biotinylated antibody, or purified antibody specific to pig-specific cell surface markers, such as CD3, CD21, CD172 (Southern Biotech), CD4, CD8, CD11c (BD Biosciences), CD25, major histocompatibility complex (MHC) class II (Serotec), TcR1N4 (VMRD), and FoxP3 (eBioscience). Respective isotype controls were also included in the assay. Cells were then washed with FACS buffer and treated with streptavidin-conjugated fluorochromes or respective anti-species isotype-specific secondary antibody conjugated with fluorochromes. Finally, cells were fixed with 1% paraformaldehyde, and immunostained cells were acquired using FACS AriaII (BD Biosciences) and analyzed using FlowJo software (Tree Star, Inc., OR). For FoxP3 staining, the cells were first surface stained for CD4 α and CD25 as described above and then fixed, permeabilized and stained with fluorochrome-conjugated pig FoxP3 cross-reactive anti-rat FoxP3 MAb as described previously, and acquired and analyzed as described above.

Lymphocyte subpopulations were separated initially by CD3-positive and -negative gates. Based on CD4 and CD8 staining characteristics, each subpopulation was then further grouped as follows: (i) lymphocyte subsets with phenotype CD3 $^+$ CD4 $^-$ CD8 $^+$ (natural killer [NK] cells) (15), CD3 $^+$ CD4 $^+$ CD8 $^-$ (T-helper cells), CD3 $^+$ CD4 $^-$ CD8 $^+$ [cytotoxic T lymphocytes (CTL)] and CD3 $^+$ CD4 $^+$ CD8 $^+$ (T-helper/memory phenotype) (41), (ii) regulatory T cells (Tregs) (CD4 $^+$ CD25 $^+$ Foxp3 $^+$), (iii) $\gamma\delta$ T cells (CD8 α^+ TcR1N4 $^+$), (iv) B cells (CD21 $^+$), and (v) activated T cells (CD3 $^+$ CD25 $^+$). All the CD172 $^+$ cells were grouped as a total myeloid cell population, and cells with CD172 $^+$ CD11c $^+$ MHC class II $^+$ were grouped as a dendritic cell (DC)-rich fraction. Frequencies of individual lymphocyte and myeloid cell subsets were analyzed from 50,000 to 100,000 total events. Data are presented as a fold change in the frequencies of cell subsets from SwIV-infected pigs over that of the control.

Influenza virus-specific memory immune responses. The assay to measure the recall/memory cytokine response was performed as described previously (46) with few modifications. Briefly, five million TBLN-MNC of pigs infected with SwIV OH07 at PID 6 were restimulated with the inactivated total SwIV OH07 antigens (100 $\mu\text{g}/\text{ml}$) for 72 h at 37°C in an enriched RPMI 1640 (E-RPMI) (10% FBS, gentamicin [100 $\mu\text{g}/\text{ml}$], ampicillin [20 $\mu\text{g}/\text{ml}$], 20 mM HEPES, 2 mM L-glutamine, 0.1 mM nonessential amino acids, 1 mM sodium pyruvate, and 50 nM 2-ME) in 24-well tissue culture plates. IFN- γ production in the supernatants was measured by ELISA as described above.

Statistical analysis. Mean body temperatures, extent of gross and histopathologic changes, and virus replication in both infected and control groups were compared using the two-sided Student's *t* test. *P* values of <0.05 were considered to indicate a statistically significant difference between the pig groups.

RESULTS

SwIV-infected pigs had clinical disease with severe acute lung pathology. In pigs, rectal temperatures of $\geq 103^\circ\text{F}$ are considered a febrile response. Pigs inoculated with SwIV OH07 (SwIV) had a constant elevated febrile response from PIDs 1 to 5, while control pigs remained afebrile (data not shown). Three out of six SwIV-infected pigs had nasal dis-

charge at PID 1. During necropsy, gross purple-red consolidated pulmonary lesions typical of SwIV were observed in the infected pigs; these lesions were not present in the control pigs (Fig. 1A). The affected part of the lungs exhibited a lobular pattern and was depressed from the adjacent normal lung parenchyma. The mean percent gross lung lesion scores in infected pigs were 28 ± 13.4 and 30 ± 15.9 at PIDs 3 and 6, respectively (Fig. 1B). Microscopically, the inflammatory changes observed in lungs of SwIV-infected pigs reflected the gross lesions. In SwIV-infected pigs, bronchial epithelial cell hyperplasia (multiple epithelial cell layers, admixed with clear evidence of epithelial cell necrosis) and extensive intraluminal aggregates of necrotic debris and inflammatory cell infiltrates were observed [Fig. 1C (ii)]. In severely infected pig lungs, the bronchi were completely denuded of lining epithelium. Interstitial pneumonia was characterized by thickening of alveolar walls with infiltrated inflammatory cells and collapsed alveolar spaces [Fig. 1C (iv)].

Replication of SwIV was detected principally in the pig lung. Virus shedding into the nasal cavity peaked at PID 1 ($10^{5.2}$ TCID $_{50}/\text{ml}$), and infectious virus was recovered until PID 6 (Table 1). SwIV replication was detected in all the lung lobes of both right and left lungs (Table 1). Virus titers varied among infected pigs, and in particular the highest titer observed was in the left caudal lobe at both PIDs 3 and 6. In the trachea, virus replication was detected at both PIDs 3 (titer range, $10^{2.75}$ to $10^{4.5}/\text{ml}$) and 6 (titer range, $10^{2.5}$ to $10^{4.25}/\text{ml}$). Interestingly, virus replication was not detected in any other nonrespiratory organ, except in tonsils, where two of three pigs at both the PIDs had a titer of $10^{1.5}/\text{ml}$ (the minimum detection limit of the assay). These results indicated that SwIV virus replicates mainly in the pig lungs.

Humoral immune response to SwIV. SwIV-infected pigs had significantly higher levels of anti-SwIV-specific IgA antibodies in their lungs than controls at both PIDs 3 and 6 (Fig. 2). Virus-specific IgG and IgM antibody responses were not detected in the lungs of infected pigs at either of the time points tested (data not shown).

SwIV infection induces the proinflammatory cytokine response in the lungs. The amount of secreted IFN- α was significantly higher at PID 3 in the SwIV-infected pig lungs than in the respective mock-infected control (Fig. 3A). The concentrations of IL-6 and IL-12 were higher at both PIDs 3 and 6 (Fig. 3B and D) in the lungs of SwIV-infected pigs. In addition, substantially larger amounts of IFN- γ were detected in the lungs of SwIV-infected pigs than controls at PID 6 (Fig. 3C). The concentrations of IL-10, TGF- β , and IL-4 in virus-infected pigs were slightly higher than those in control pig lungs at both the PIDs (data not shown). Small amounts of TNF- α were also detected in the SwIV-infected pig lungs at PID 3 but not in controls (data not shown).

SwIV infection altered the frequency of both lymphoid and myeloid cells in the pig lungs. The immune cell phenotypes in the SwIV-infected pig lungs were analyzed early in the infection (PID 3) and also when cells are expected to infiltrate in to the lungs (PID 6). Virus infection led to a decrease in the frequency of NK cells in lungs and PBMC at both the PIDs in BAL fluid, tonsils, and PBMC (Fig. 4A). At PID 3, the frequency of the DC-rich population was substantially increased in the lungs and tonsils but decreased in TBLN and blood,

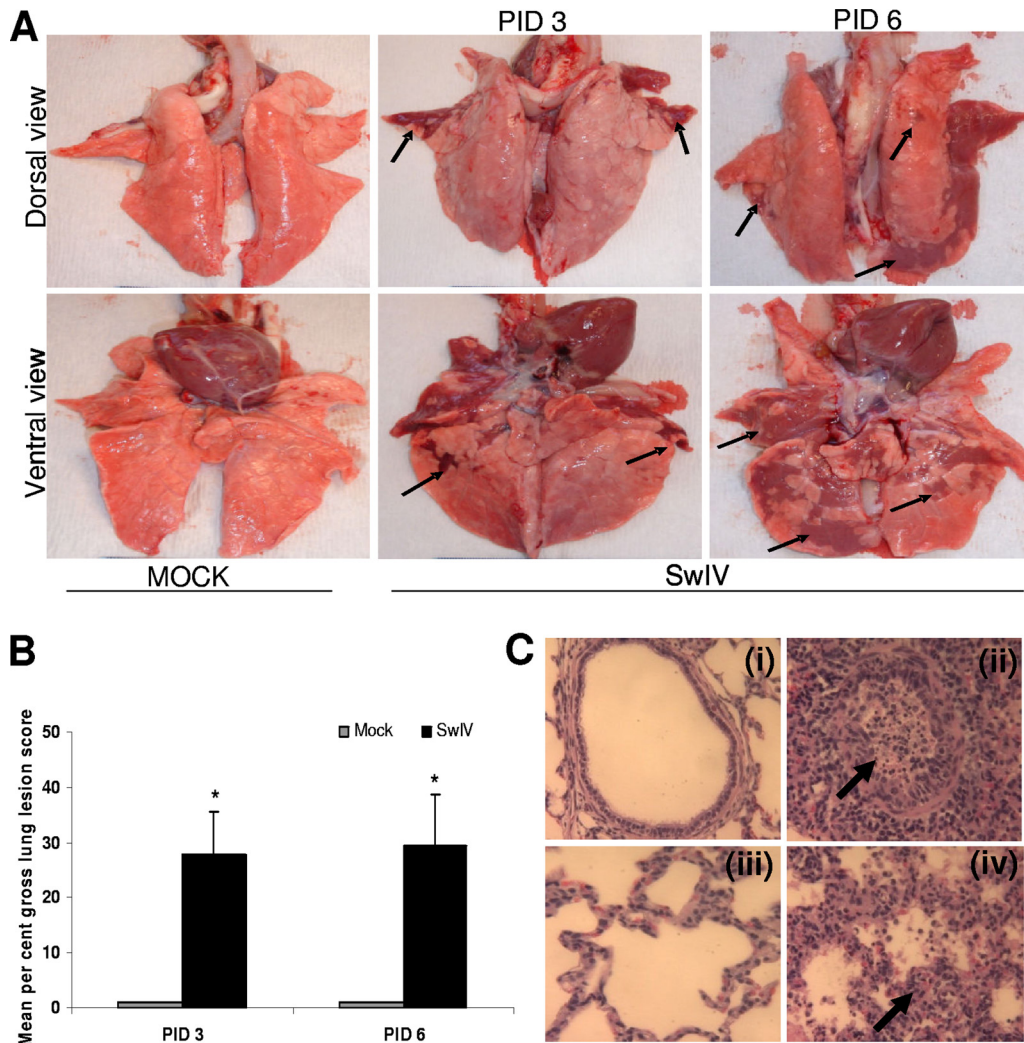


FIG. 1. Gross lung lesions in pigs infected with SwIV OH07. (A) Five-week-old pigs were mock infected or infected with SwIV. At PIDs 3 and 6, extensive areas of purple-red consolidation indicative of severe pneumonia were observed in lungs of virus-infected pigs. (B) Mean gross lung lesions from all the six lung lobes were scored on the basis of percent pneumonic lesions. Virus-infected pigs had significantly higher ($P < 0.05$) mean lung lesions than mock-infected pigs at both PIDs 3 and 6. Each bar indicates the mean lung lesion scores of three pigs \pm standard error of the mean (SEM). Asterisk indicates significant differences ($P < 0.05$) in virus-infected pig lungs compared to mock-infected control pigs. Arrows indicate the purple-red consolidation in virus-infected pig lungs. A representative control and SwIV-infected pig lung is shown. (C) Microscopic lung lesions in pigs infected with SwIV OH07. Control uninfected pig lung showing normal bronchial epithelial lining and absence of inflammatory cell infiltrates and debris in the lumen (panel i). SwIV-induced bronchiolitis at PID 3 characterized by bronchial epithelial necrosis, numerous intraepithelial leukocytes, and subepithelial and peribronchial mononuclear inflammatory cell infiltrations. The bronchial lumen contains desquamated bronchial epithelium and dead and dying inflammatory cells, mainly neutrophils and proteinic debris, indicated by an arrow (panel ii). Panel iii shows control uninfected lung, showing normal alveolar walls, clear air space, and absence of exudation into the alveolar space. Panel iv shows SwIV-induced exudative interstitial pneumonia at PID 3, illustrating the thickened alveolar walls containing intravascular and extravascular inflammatory cells, indicated by an arrow. The alveolar spaces are collapsed and contain proteinic debris and an increased population of inflammatory cells. Hematoxylin and eosin stain. Magnification, $\times 200$. Representative control and SwIV-infected pig lung sections are shown. Similar histological changes were detected in pig lungs of another independent experiment.

whereas at PID 6, the DC-rich fraction was much higher in the lungs, BAL fluid, and PBMC than that in mock-control pigs (Fig. 4B). A slight increase in the total B cells in BAL fluid and a decrease in the TBLN and tonsils were detected for the infected pigs at PID 3. At PID 6, their frequency was lower in BAL fluid ($10.7 \pm 1.0\%$ in controls versus $3.1 \pm 0.8\%$ in infected pigs; $P < 0.05$) and substantially higher in the tonsils than the respective levels in control pigs (Fig. 4C).

In SwIV-infected pigs, a significant reduction in the propor-

tion of $CD4^+$ T cells (T-helper cells) in TBLN ($52.4 \pm 4.4\%$ in controls versus $32.2 \pm 4.6\%$ in infected pigs; $P < 0.05$) and a substantial decrease of these cells in the lungs, tonsils, and PBMC at PID 3 was detected. However, the frequency of $CD4^+$ T cells was increased substantially in BAL fluid and tonsils and even more significantly ($37.2 \pm 4.2\%$ in controls versus $50.2 \pm 1.0\%$ in infected pigs) in PBMC compared to that in control pigs at PID 6 (Fig. 4D). CTLs were substantially higher in the frequency in TBLN and tonsils at PID 3 and

TABLE 1. Virus titers in nasal swabs and lungs from infected pigs^a

PID	Virus titer (log ₁₀ TCID ₅₀ /ml) in:						
	Nasal swabs	Left lung lobes			Right lung lobes		
		Cranial	Caudal	Accessory	Cranial	Middle	Caudal
1	5.20 ± 0.29						
2	4.83 ± 0.33						
3	5.00 ± 0.36	5.26 ± 0.49	7.33 ± 0.44	3.12 ± 3.12	5.48 ± 0.41	4.98 ± 0.24	2.66 ± 1.58
4	4.83 ± 0.33						
5	4.50 ± 0.00						
6	1.16 ± 0.60	4.18 ± 1.35	5.00 ± 0.25	4.08 ± 0.30	3.40 ± 1.15	3.75 ± 0.80	3.50 ± 1.01

^a Five-week-old pigs were infected with Sw/OH/24366/07 H1N1 virus. Nasal swabs were collected daily up to PID 6. At PIDs 3 and 6, lungs were harvested from the infected pigs and 10% homogenate was prepared from individual lung lobes by using tissue homogenizer. Influenza virus shedding in the nasal swabs and virus titers in individual lung lobes were determined by titration using MDCK cells. Values indicate mean virus titers in nasal swabs of six pigs ± SEM from PID 1 to PID 3 and three pigs ± SEM from PID 4 to PID 6 and the mean virus titers in individual lung lobes of three pigs ± SEM at PIDs 3 and 6 except in the accessory lung lobe at PID 3, where values are mean virus titers ± SEM for two pigs. A similar trend in the virus titers in nasal swabs and lungs was detected in another independent experiment.

significantly higher in lungs (17.5 ± 3.7 versus 29.3 ± 1.7) and in BAL fluid ($8.3 \pm 1.1\%$ versus $43.4 \pm 4.0\%$) in control versus infected pigs, respectively, at PID 6 (Fig. 4E). The levels of $\gamma\delta$ T cells were slightly higher in BAL fluid and lower in the TBLN of SwIV-infected pigs at PID 3 and significantly higher in BAL fluid ($3.2 \pm 0.5\%$ in controls versus $6.3 \pm 0.6\%$ in infected pigs) and lower in tonsils of the infected pigs than those of the respective control pigs (Fig. 4F).

In infected pigs, a higher frequency of Treg cells (Tregs) was detected in the lungs and tonsils, but their frequency was lower in the BAL fluid at PID 3. At PID 6, their frequency was higher in the lungs ($2.7 \pm 0.04\%$ in controls versus $8.0 \pm 0.4\%$ in infected pigs; $P < 0.05$), BAL fluid, tonsils, and PBMC than in corresponding samples from control pigs (Fig. 5A). CD4CD25FoxP3 triple positive cells (Tregs) were detected consistently in SwIV-infected pig lungs (Fig. 5B). Memory/T-helper cells were significantly higher in TBLN ($5.7 \pm 0.3\%$ in controls versus $14.6 \pm 1.1\%$ in infected pigs), BAL fluid ($0.7 \pm 0.2\%$ versus $5.4 \pm 0.9\%$), and tonsils ($3.3 \pm 1.3\%$ versus $13.5 \pm 1.7\%$) in control versus SwIV-infected pigs, respectively (Fig. 5C). At PID 6, the frequency of activated T cells was significantly higher in the lungs ($1.5 \pm 0.15\%$ versus $4.2 \pm$

0.8%) and BAL fluid ($2.0 \pm 1.0\%$ versus 5.7 ± 0.3) in control versus SwIV-infected pigs, respectively (Fig. 5D). In particular, activated T-helper cells ($CD4^+ CD25^+$) were significantly higher in BAL fluid ($1.4 \pm 0.1\%$ in controls versus $6.1 \pm 0.6\%$ in infected pigs) and substantially higher in the lungs. Activated CTLs ($CD8^+ CD25^+$) were higher in the lungs and BAL fluid ($1.9 \pm 0.1\%$ in controls versus $5.6 \pm 0.4\%$ in infected pigs; $P < 0.05$). In contrast, activated T cells were comparable to those of mock-infected pigs in TBLN and tonsils in SwIV-infected pigs (Fig. 5D).

Detection of virus-specific recall/memory T-cell response in the TBLN. The levels of IFN- γ produced by TBLN-MNC of SwIV-infected pigs upon restimulation in the presence of killed SwIV antigens were analyzed *ex vivo* and found to be

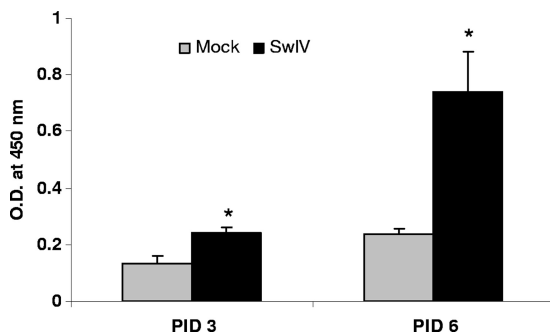


FIG. 2. SwIV-specific IgA antibody response in the lungs of experimentally infected pigs. On PIDs 3 and 6, virus-specific IgA antibody production in lungs of mock- and SwIV-infected pigs was analyzed by ELISA. Each bar indicates mean OD₄₅₀ ± SEM for three pigs. Asterisk indicates significant differences ($P < 0.05$) in virus-infected pig lungs compared to mock-infected control pigs. A similar trend in the virus-specific IgA antibody response was also found in another independent experiment.

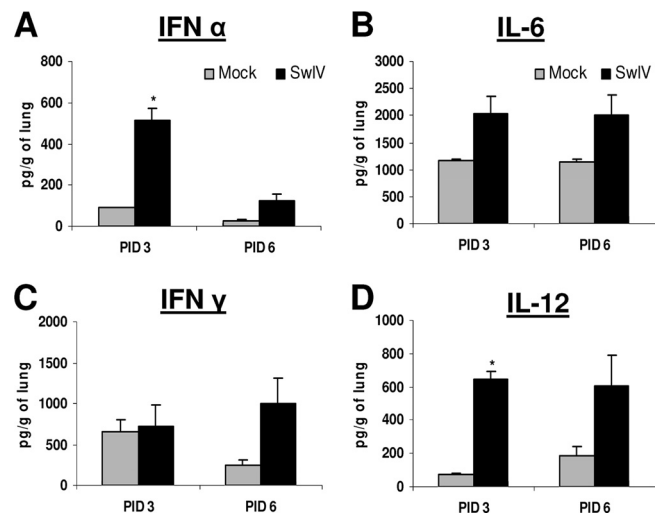


FIG. 3. Cytokine production in pig lungs infected with SwIV OH07. Five-week-old pigs were mock infected or infected intranasally and intratracheally with SwIV. At PIDs 3 and 6, cytokine production in lung lysate of mock- and virus-infected pigs was analyzed: innate (IFN- α) (A), proinflammatory (IL-6) (B), Th1 IFN- γ (C), and IL-12 cytokines (D) by ELISA. Each bar indicates mean concentrations of cytokines ± SEM for three pigs. Asterisk indicates significant differences ($P < 0.05$) in virus-infected pig lungs compared to mock-infected control pigs. A similar trend in the cytokine response was detected in another independent experiment.

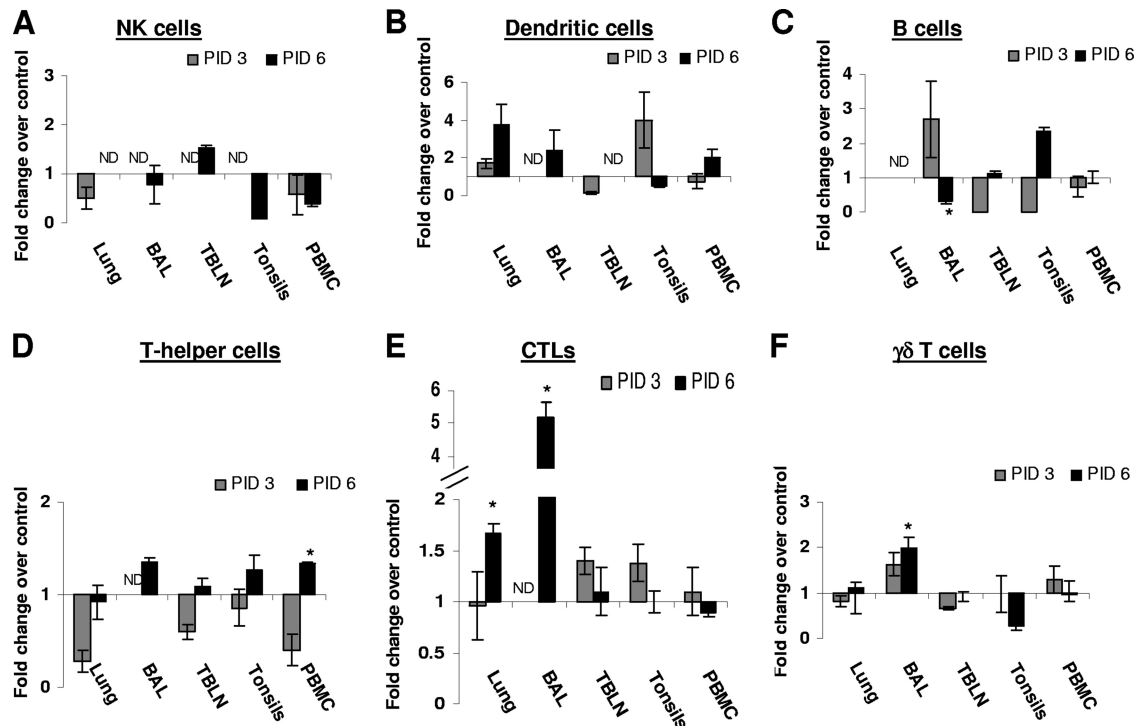


FIG. 4. Comparison of innate immune cells (NK cells and DC), B cells, and T lymphocyte subsets in different tissues of mock-infected and SwIV-infected pigs. Five-week-old pigs were mock-infected or infected with SwIV. At PIDs 3 and 6, MNC isolated from the lungs, BAL fluid, TBLN, tonsils, and PBMC were immunostained with appropriate antibodies or its isotype control MAb and then analyzed by flow cytometry for NK cells (A), DC cells (B), B cells (C), T-helper cells (D), CTLs (E), and $\gamma\delta$ T cells (F). Data shown are the fold increase or decrease in the mean ($n = 3$ pigs/group) percentage of indicated pig immune cells of SwIV versus those of mock-infected pigs. A similar trend in the frequency of immune cells was detected in another independent experiment.

significantly higher at PID 6 than those of mock-infected control pigs (Fig. 6).

DISCUSSION

The goal of the present study was to examine the pathogenesis of H1N1 SwIV OH07 (SwIV) in the natural host with particular emphasis on the host mucosal immune responses. This study is the first to demonstrate the phenotype of different immune cells associated with innate, adaptive, and regulatory immune responses during the acute phase of the disease, in particular at the site of viral replication. Originally, SwIV was isolated from pigs, the virus was transmitted to humans, and the same virus was recovered from patients (43, 55). Consistent with a previous study (51), we also detected nasal shedding of SwIV and observed extensive lung lesions. In addition, we detected replication of the virus to a higher titer in the lungs and the virus was not detected in other tissues, suggesting the lack of tissue tropism in other organs. Consistent with H1N1 SwIV, pandemic H1N1 influenza virus also replicated predominantly in the lungs and not in any other pig organs (5). Interestingly, the SwIV OH07-induced lung lesions in pigs were more severe than those induced by U.S. H1N1 SwIV (49).

Cellular immune responses are critical for the complete clearance of the influenza virus (18). SwIV-infected pigs had a higher frequency of CD8⁺ T cells in TBLN, BAL fluid, tonsils, and lungs, indicating the proliferation of influenza-specific CD8⁺ T cells. In influenza virus-infected mice, CD8⁺ T cells

continued to proliferate even after they migrated to the lungs, contributing significantly toward the antiviral immunity (32). Increased CD8⁺ T cells in BAL fluid and blood of H1N1 and pandemic H1N1 influenza virus-infected pigs was detected (21, 27). Apart from helping in viral clearance, the CD8⁺ T cells have been the major effectors for mediating heterotypic immunity against influenza viruses (14, 21, 26, 35, 42). In contrast, the frequencies of CD4⁺ T cells were decreased initially in tonsils, TBLN, blood, and lungs but increased substantially at PID 6. Similarly, an increase in the frequency of CD4⁺ T cells in BAL fluid and PBMC of pandemic H1N1 influenza virus-infected pigs was observed at PID 6 (27). Presumably, the role of CD4⁺ T cells in mediating the recovery from influenza virus infection is by stimulating the generation of antiviral neutralizing antibodies (33, 45) and by providing necessary help for the proliferation of virus-specific CTLs (37). Consistent with that, an increased frequency of activated CD4⁺ T cells associated with enhanced generation of the SwIV-specific mucosal IgA and an increased frequency of activated CD8⁺ T cells in pig lungs were detected. Activated CD4⁺ CD8⁺ T cells in pigs possess T-helper, cytolytic, and memory properties, important for the viral clearance (12). Interestingly, in SwIV-infected BAL fluid, TBLN, and tonsils, significantly higher frequencies of CD4⁺ CD8⁺ T cells were detected. Consistent with our results, elevated levels of CD4⁺ CD8⁺ T cells were also detected in the blood of pandemic H1N1 virus-infected pigs (27).

The frequency of NK cells in lungs, BAL fluid, and PBMC

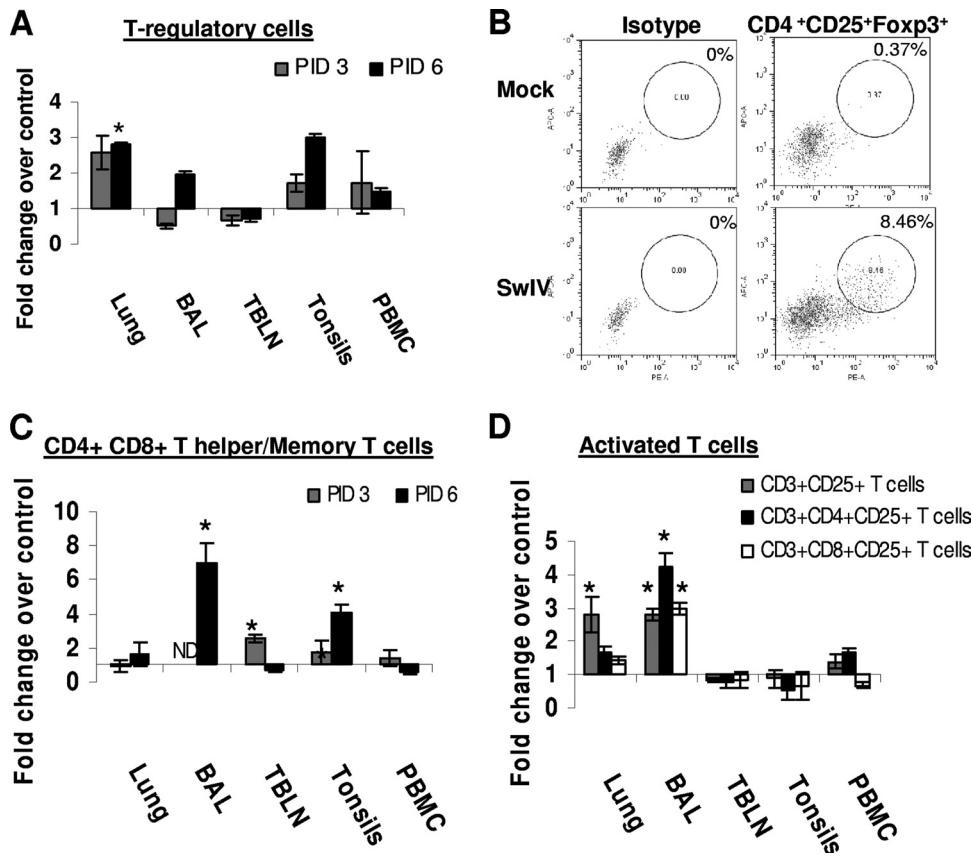


FIG. 5. Frequency of T regulatory cells, T-helper/memory cells, and activated T cells in SwIV-infected pigs. Five-week-old pigs were mock infected or infected with SwIV. At PIDs 3 and 6, MNC isolated from the lungs, BAL fluid, TBLN, tonsils, and PBMC were immunostained with appropriate antibodies or its isotype control MAb and then analyzed by flow cytometry for T regulatory cells (CD4⁺ CD25⁺ Foxp3⁺) (A and B), CD4⁺ CD8⁺ T helper/memory T cells (C), and activated T cells (D) at PID 6. Data shown are the fold increase or decrease in the mean ($n = 3$ pigs/group) percentage of immune cells of SwIV over those of mock-infected pigs. A representative dot plot of results for a mock- and an SwIV-infected pig showing the frequency of Tregs in the pig lungs at PID 6 is shown (B). Asterisk indicates significant differences ($P < 0.05$) in the SwIV- versus mock-infected pig immune cells. A similar trend in these immune cells was detected in another independent experiment.

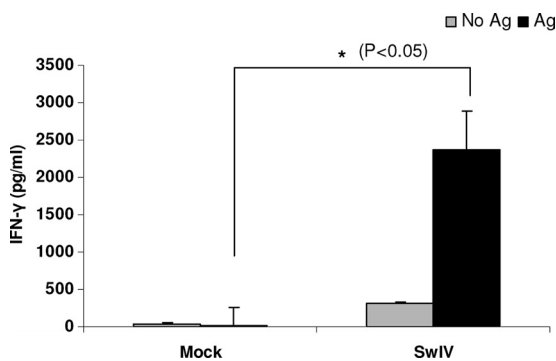


FIG. 6. IFN- γ production by *in vivo* SwIV OH07 primed pig lymphocytes of TBLN upon *ex vivo* restimulation. TBLN-MNC of mock- and SwIV-infected pigs at PID 6 were restimulated *ex vivo* in the presence of inactivated SwIV antigens. IFN- γ production in the supernatant was measured by ELISA. Each bar indicates the mean IFN- γ concentration \pm SEM for three pigs. Asterisk indicates significant differences ($P < 0.05$) in the amount of IFN- γ secreted by SwIV- versus mock-infected pig cells. Similar results were also found in another independent experiment.

was decreased in SwIV-infected pigs. However, elevated levels of NK cells in BAL fluid up to PID 15 in influenza virus-infected pigs were shown by others (21). The likely reasons for this discrepancy include differences in the timing of sample collection, the strain of the virus used, the animal age, the route of virus inoculation, and the dose of the virus used to infect pigs. However, consistent with our results, humans suffering from severe influenza virus infection showed diminished NK cells in the blood and lungs (22, 53). It was also demonstrated that influenza virus infection causes lysis and apoptosis of NK cells in humans (31).

In lungs of SwIV-infected pigs, a higher frequency of DC-rich fraction was detected. Matured DC produce IL-12 (11), and, incidentally, larger amounts of IL-12 in pig lungs were also detected in our study. The cytokine IL-12 produced by DC activates NK cells and stimulates the production of IFN- γ by antigen-specific T cells. Consistent with this, an increased amount of IFN- γ was detected in the lungs of SwIV-infected pigs, suggesting possible secretion of IFN- γ by activated CD4⁺ and CD8⁺ T cells. IFN- γ secretion is widely used for the assessment of antigen-specific Th1 immune responses in swine (56), humans, and other animal species. In our study, IFN- γ

was secreted by lymphocytes of TBLN of SwIV-infected pigs, suggesting that activated T cells were present in the infected pigs.

In mice with influenza virus A infection, an increased frequency of $\gamma\delta$ T cells during the recovery phase of the disease was detected (13). $\gamma\delta$ T cells provide protection at mucosal surfaces (6), they are phagocytic, and they are involved in the antigen presentation in conjunction with MHC class II molecules in humans (54). Consistent with that, a significant increase in the proportion of $\gamma\delta$ T cells in the lungs and BAL fluid of pigs infected with SwIV was observed in our study; however, their incipient APC function was not tested.

Tregs are known to mediate anti-inflammatory immune responses (30) and play an important role in the pathogenesis of certain viral infections which cause severe inflammatory lesions, such as influenza. We detected a significantly higher frequency of Tregs in SwIV-infected pig lungs, suggesting an attempt by the host to downregulate the severe inflammatory response mediated by the SwIV. One way Tregs mediate strong immunosuppressive responses is by secreting the cytokine IL-10 (25). Consistent with that, higher levels of the anti-inflammatory cytokines IL-10 and TGF- β were detected in SwIV-infected pig lungs. In humans, an increase in the frequency of Tregs was detected following pandemic H1N1 infection (16). In a model of virus-induced inflammatory disease caused by a herpes simplex virus infection of the mouse cornea, Tregs attenuated the disease severity by modulating T cell-mediated inflammatory responses (44).

In summary, SwIV OH07 replicated extensively and exclusively in pig lungs, and virus replication in the lungs was accompanied by clinical disease with severe pulmonary inflammation. In the infected pig lungs, secretion of innate, proinflammatory, Th1, Th2, and Th3 cytokines was detected. In addition, a strong mucosal SwIV-specific IgA antibody response, activated T helper cells, CTLs, and Tregs were detected in the pig lungs. Due to the striking similarities between the pathogenesis of SwIV OH07 in pigs and that of pandemic H1N1 virus in humans, the swine SwIV OH07 infection model could be useful for pandemic H1N1 virus pathogenesis studies. Based on our results, we strongly believe that the pig may serve as a useful animal model to design and test effective vaccines and therapeutics against pandemic-influenza-induced pneumonia. Future studies will be directed to delineate the role of individual immune cell subsets in the pathogenesis of influenza virus in pigs.

ACKNOWLEDGMENTS

We thank Ruthi Patterson, Katie Dodson, and Megan Strother for technical assistance and Juliette Hanson, Kingsly Berlin, and Todd Root for assistance with animal care. We also thank Kwonil Jung for his help with initial lung lesion scoring. We also thank Michele Williams for editing the manuscript.

We have no financial conflict of interest.

REFERENCES

- Azevedo, M. S., L. Yuan, S. Pouly, A. M. Gonzales, K. I. Jeong, T. V. Nguyen, and L. J. Saif. 2006. Cytokine responses in gnotobiotic pigs after infection with virulent or attenuated human rotavirus. *J. Virol.* **80**:372–382.
- Barbe, F., K. Atanasova, and K. Van Reeth. 2010. Cytokines and acute phase proteins associated with acute swine influenza infection in pigs. *Vet. J.* doi:10.1016/j.tvjl.2009.12.012.
- Reference deleted.
- Basta, S., C. P. Carrasco, S. M. Knoetig, R. C. Rigden, H. Gerber, A. Summerfield, and K. C. McCullough. 2000. Porcine alveolar macrophages: poor accessory or effective suppressor cells for T-lymphocytes. *Vet. Immunol. Immunopathol.* **77**:177–190.
- Brookes, S. M., A. Nunez, B. Choudhury, M. Matrosovich, S. C. Essen, D. Clifford, M. J. Slomka, G. Kuntz-Simon, F. Garcon, B. Nash, A. Hanna, P. M. Heegaard, S. Queguiner, C. Chiapponi, M. Bublot, J. M. Garcia, R. Gardner, E. Foni, W. Loeffen, L. Larsen, K. Van Reeth, J. Banks, R. M. Irvine, and I. H. Brown. 2010. Replication, pathogenesis and transmission of pandemic (H1N1) 2009 virus in non-immune pigs. *PLoS One* **5**:e9068.
- Carding, S. R., and P. J. Egan. 2002. Gammadelta T cells: functional plasticity and heterogeneity. *Nat. Rev. Immunol.* **2**:336–345.
- Charley, B. 1977. Local immunity in the pig respiratory tract. I. Cellular and humoral immune responses following swine influenza infection. *Ann. Microbiol. (Paris)* **128B**:95–107.
- Choi, H. K., W. E. Finkbeiner, and J. H. Widdicombe. 2000. A comparative study of mammalian tracheal mucous glands. *J. Anat.* **197**(Pt. 3):361–372.
- Cozzi, E., A. W. Tucker, G. A. Langford, G. Pino-Chavez, L. Wright, M. J. O'Connell, V. J. Young, R. Lancaster, M. McLaughlin, K. Hunt, M. C. Bordin, and D. J. White. 1997. Characterization of pigs transgenic for human decay-accelerating factor. *Transplantation* **64**:1383–1392.
- Cunningham, S., Q. H. Meng, N. Klein, R. J. McAnulty, and S. L. Hart. 2002. Evaluation of a porcine model for pulmonary gene transfer using a novel synthetic vector. *J. Gene Med.* **4**:438–446.
- Dalod, M., T. P. Salazar-Mather, L. Malmgaard, C. Lewis, C. Asselin-Paturel, F. Briere, G. Trinchieri, and C. A. Biron. 2002. Interferon alpha/beta and interleukin 12 responses to viral infections: pathways regulating dendritic cell cytokine expression in vivo. *J. Exp. Med.* **195**:517–528.
- De Bruin, T. G., E. M. Van Rooij, Y. E. De Visser, and A. T. Bianchi. 2000. Cytolytic function for pseudorabies virus-stimulated porcine CD4+ CD8dull+ lymphocytes. *Viral Immunol.* **13**:511–520.
- Doherty, P. C., W. Allan, D. B. Boyle, B. E. Coupar, and M. E. Andrew. 1989. Recombinant vaccinia viruses and the development of immunization strategies using influenza virus. *J. Infect. Dis.* **159**:1119–1122.
- Furuya, Y., J. Chan, M. Regner, M. Lobigs, A. Koskinen, T. Kok, J. Manavis, P. Li, A. Mullbacher, and M. Alsharif. 2010. Cytotoxic T cells are the predominant players providing cross-protective immunity induced by γ -irradiated influenza A viruses. *J. Virol.* **84**:4212–4221.
- Gerner, W., T. Kaser, and A. Saalmuller. 2009. Porcine T lymphocytes and NK cells—an update. *Dev. Comp. Immunol.* **33**:310–320.
- Giamarellos-Bourboulis, E. J., M. Raftogiannis, A. Antonopoulou, F. Baziaka, P. Koutoukas, A. Savva, T. Kanni, M. Georgitsi, A. Pistiki, T. Tsaganos, N. Pelekanos, S. Athanassia, L. Galani, E. Giannitsioti, D. Kavatha, F. Kontopidou, M. Mouktaroudi, G. Poulakou, V. Sakka, P. Panagopoulos, A. Papadopoulos, K. Kanellakopoulou, and H. Giamarellou. 2009. Effect of the novel influenza A (H1N1) virus in the human immune system. *PLoS One* **4**:e8393.
- Goco, R. V., M. B. Kress, and O. C. Brantigan. 1963. Comparison of mucus glands in the tracheobronchial tree of man and animals. *Ann. N. Y. Acad. Sci.* **106**:555–571.
- Graham, M. B., and T. J. Braciale. 1997. Resistance to and recovery from lethal influenza virus infection in B lymphocyte-deficient mice. *J. Exp. Med.* **186**:2063–2068.
- Halbur, P. G., P. S. Paul, M. L. Frey, J. Landgraf, K. Eernisse, X. J. Meng, M. A. Lum, J. J. Andrews, and J. A. Rathje. 1995. Comparison of the pathogenicity of two US porcine reproductive and respiratory syndrome virus isolates with that of the Lelystad virus. *Vet. Pathol.* **32**:648–660.
- Hayden, F. G., R. Fritz, M. C. Lobo, W. Alvord, W. Strober, and S. E. Straus. 1998. Local and systemic cytokine responses during experimental human influenza A virus infection. Relation to symptom formation and host defense. *J. Clin. Invest.* **101**:643–649.
- Heinen, P. P., E. A. de Boer-Luijtz, and A. T. Bianchi. 2001. Respiratory and systemic humoral and cellular immune responses of pigs to a heterosubtypic influenza A virus infection. *J. Gen. Virol.* **82**:2697–2707.
- Heltzer, M. L., S. E. Coffin, K. Maurer, A. Bagashev, Z. Zhang, J. S. Orange, and K. E. Sullivan. 2009. Immune dysregulation in severe influenza. *J. Leukoc. Biol.* **85**:1036–1043.
- Ibrahim, Z., J. Busch, M. Awwad, R. Wagner, K. Wells, and D. K. Cooper. 2006. Selected physiologic compatibilities and incompatibilities between human and porcine organ systems. *Xenotransplantation* **13**:488–499.
- Jung, K., G. J. Renukaradhya, K. P. Alekseev, Y. Fang, Y. Tang, and L. J. Saif. 2009. Porcine reproductive and respiratory syndrome virus modifies innate immunity and alters disease outcome in pigs subsequently infected with porcine respiratory coronavirus: implications for respiratory viral coinfections. *J. Gen. Virol.* **90**:2713–2723.
- Kaser, T., W. Gerner, S. E. Hammer, M. Patzl, and A. Saalmuller. 2008. Phenotypic and functional characterisation of porcine CD4(+)CD25(high) regulatory T cells. *Vet. Immunol. Immunopathol.* **122**:153–158.
- Kreijtz, J. H., R. Bodewes, G. van Amerongen, T. Kuiken, R. A. Fouchier, A. D. Osterhaus, and G. F. Rimmelzwang. 2007. Primary influenza A virus infection induces cross-protective immunity against a lethal infection with a heterosubtypic virus strain in mice. *Vaccine* **25**:612–620.
- Lange, E., D. Kalthoff, U. Blohm, J. P. Teifke, A. Breithaupt, C. Maresch, E.

- Starick, S. Fereidouni, B. Hoffmann, T. C. Mettenleiter, M. Beer, and T. W. Vahlenkamp. 2009. Pathogenesis and transmission of the novel swine-origin influenza virus A/H1N1 after experimental infection of pigs. *J. Gen. Virol.* **90**:2119–2123.
28. Lee, B. W., R. F. Bey, M. J. Baarsch, and M. E. Larson. 1995. Class specific antibody response to influenza A H1N1 infection in swine. *Vet. Microbiol.* **43**:241–250.
29. Loving, C. L., S. L. Brockmeier, and R. E. Sacco. 2007. Differential type I interferon activation and susceptibility of dendritic cell populations to porcine arterivirus. *Immunology* **120**:217–229.
30. Majlessi, L., R. Lo-Man, and C. Leclerc. 2008. Regulatory B and T cells in infections. *Microbes Infect.* **10**:1030–1035.
31. Mao, H., W. Tu, G. Qin, H. K. Law, S. F. Sia, P. L. Chan, Y. Liu, K. T. Lam, J. Zheng, M. Peiris, and Y. L. Lau. 2009. Influenza virus directly infects human natural killer cells and induces cell apoptosis. *J. Virol.* **83**:9215–9222.
32. McGill, J., and K. L. Legge. 2009. Cutting edge: contribution of lung-resident T cell proliferation to the overall magnitude of the antigen-specific CD8 T cell response in the lungs following murine influenza virus infection. *J. Immunol.* **183**:4177–4181.
33. Mozdzanowska, K., M. Furchner, K. Maiese, and W. Gerhard. 1997. CD4+ T cells are ineffective in clearing a pulmonary infection with influenza type A virus in the absence of B cells. *Virology* **239**:217–225.
34. Myers, K. P., S. F. Setterquist, A. W. Capuano, and G. C. Gray. 2007. Infection due to 3 avian influenza subtypes in United States veterinarians. *Clin. Infect. Dis.* **45**:4–9.
35. Nguyen, H. H., Z. Moldoveanu, M. J. Novak, F. W. van Ginkel, E. Ban, H. Kiyono, J. R. McGhee, and J. Mestecky. 1999. Heterosubtypic immunity to lethal influenza A virus infection is associated with virus-specific CD8(+) cytotoxic T lymphocyte responses induced in mucosa-associated tissues. *Virology* **254**:50–60.
36. Renukaradhya, G. J., K. P. Alekseev, K. Jung, F. Fang, and L. J. Saif. 2010. Porcine reproductive and respiratory syndrome virus induced immunosuppression exacerbate the inflammatory response to porcine respiratory coronavirus in pigs. *Viral Immunol.* **24**:457–466.
37. Riberdy, J. M., K. J. Flynn, J. Stech, R. G. Webster, J. D. Altman, and P. C. Doherty. 1999. Protection against a lethal avian influenza A virus in a mammalian system. *J. Virol.* **73**:1453–1459.
38. Richt, J. A., K. M. Lager, B. H. Janke, R. D. Woods, R. G. Webster, and R. J. Webby. 2003. Pathogenic and antigenic properties of phylogenetically distinct reassortant H3N2 swine influenza viruses cocirculating in the United States. *J. Clin. Microbiol.* **41**:3198–3205.
39. Rogers, C. S., W. M. Abraham, K. A. Brogden, J. F. Engelhardt, J. T. Fisher, P. B. McCray, Jr., G. McLennan, D. K. Meyerholz, E. Namati, L. S. Ostedgaard, R. S. Prather, J. R. Sabater, D. A. Stoltz, J. Zabner, and M. J. Welsh. 2008. The porcine lung as a potential model for cystic fibrosis. *Am. J. Physiol. Lung Cell. Mol. Physiol.* **295**:L240–L263.
40. Rogers, C. S., D. A. Stoltz, D. K. Meyerholz, L. S. Ostedgaard, T. Rokhlina, P. J. Taft, M. P. Rogan, A. A. Pezzullo, P. H. Karp, O. A. Itani, A. C. Kabel, C. L. Wohlford-Lenane, G. J. Davis, R. A. Hanfland, T. L. Smith, M. Samuel, D. Wax, C. N. Murphy, A. Rieke, K. Whitworth, A. Uc, T. D. Starner, K. A. Brogden, J. Shilyansky, P. B. McCray, Jr., J. Zabner, R. S. Prather, and M. J. Welsh. 2008. Disruption of the CFTR gene produces a model of cystic fibrosis in newborn pigs. *Science* **321**:1837–1841.
41. Saalmuller, A., T. Pauly, B. J. Hohlich, and E. Pfaff. 1999. Characterization of porcine T lymphocytes and their immune response against viral antigens. *J. Biotechnol.* **73**:223–233.
42. Sambhara, S., A. Kurichh, R. Miranda, T. Tumpey, T. Rowe, M. Renshaw, R. Arpino, A. Tamane, A. Kandil, O. James, B. Underdown, M. Klein, J. Katz, and D. Burt. 2001. Heterosubtypic immunity against human influenza A viruses, including recently emerged avian H5 and H9 viruses, induced by FLU-ISCOM vaccine in mice requires both cytotoxic T-lymphocyte and macrophage function. *Cell. Immunol.* **211**:143–153.
43. Shinde, V., C. B. Bridges, T. M. Uyeki, B. Shu, A. Balish, X. Xu, S. Lindstrom, L. V. Gubareva, V. Deyde, R. J. Garten, M. Harris, S. Gerber, S. Vagasky, F. Smith, N. Pascoe, K. Martin, D. Duffy, K. Ritger, C. Conover, P. Quinlisk, A. Klimov, J. S. Bresee, and L. Finelli. 2009. Triple-reassortant swine influenza A (H1) in humans in the United States, 2005–2009. *N. Engl. J. Med.* **360**:2616–2625.
44. Suvas, S., A. K. Azkur, B. S. Kim, U. Kumaraguru, and B. T. Rouse. 2004. CD4+CD25+ regulatory T cells control the severity of viral immunoinflammatory lesions. *J. Immunol.* **172**:4123–4132.
45. Topham, D. J., and P. C. Doherty. 1998. Clearance of an influenza A virus by CD4+ T cells is inefficient in the absence of B cells. *J. Virol.* **72**:882–885.
46. Tsuji, N., T. Miyoshi, M. K. Islam, T. Isobe, S. Yoshihara, T. Arakawa, Y. Matsumoto, and Y. Yokomizo. 2004. Recombinant *Ascaris* 16-kilodalton protein-induced protection against *Ascaris suum* larval migration after intranasal vaccination in pigs. *J. Infect. Dis.* **190**:1812–1820.
47. VanCott, J. L., T. A. Brim, R. A. Simkins, and L. J. Saif. 1993. Isotype-specific antibody-secreting cells to transmissible gastroenteritis virus and porcine respiratory coronavirus in gut- and bronchus-associated lymphoid tissues of suckling pigs. *J. Immunol.* **150**:3990–4000.
48. Van Reeth, K., S. Van Gucht, and M. Pensaert. 2002. Correlations between lung proinflammatory cytokine levels, virus replication, and disease after swine influenza virus challenge of vaccination-immune pigs. *Viral Immunol.* **15**:583–594.
49. Vincent, A. L., K. M. Lager, W. Ma, P. Lekcharoensuk, M. R. Gramer, C. Loiacono, and J. A. Richt. 2006. Evaluation of hemagglutinin subtype 1 swine influenza viruses from the United States. *Vet. Microbiol.* **118**:212–222.
50. Vincent, A. L., W. Ma, K. M. Lager, B. H. Janke, and J. A. Richt. 2008. Swine influenza viruses: a North American perspective. *Adv. Virus Res.* **72**:127–154.
51. Vincent, A. L., S. L. Swenson, K. M. Lager, P. C. Gauger, C. Loiacono, and Y. Zhang. 2009. Characterization of an influenza A virus isolated from pigs during an outbreak of respiratory disease in swine and people during a county fair in the United States. *Vet. Microbiol.* **137**:51–59.
52. Webster, R. G., W. J. Bean, O. T. Gorman, T. M. Chambers, and Y. Kawaoka. 1992. Evolution and ecology of influenza A viruses. *Microbiol. Rev.* **56**:152–179.
53. Welliver, T. P., R. P. Garofalo, Y. Hosakote, K. H. Hintz, L. Avendano, K. Sanchez, L. Velozo, H. Jafri, S. Chavez-Bueno, P. L. Ogra, L. McKinney, J. L. Reed, and R. C. Welliver, Sr. 2007. Severe human lower respiratory tract illness caused by respiratory syncytial virus and influenza virus is characterized by the absence of pulmonary cytotoxic lymphocyte responses. *J. Infect. Dis.* **195**:1126–1136.
54. Wu, Y., W. Wu, W. M. Wong, E. Ward, A. J. Thrasher, D. Goldblatt, M. Osman, P. Digard, D. H. Canaday, and K. Gustafsson. 2009. Human gamma delta T cells: a lymphoid lineage cell capable of professional phagocytosis. *J. Immunol.* **183**:5622–5629.
55. Yassine, H. M., M. Khatri, Y. J. Zhang, C. W. Lee, B. A. Byrum, J. O'Quin, K. A. Smith, and Y. M. Saif. 2009. Characterization of triple reassortant H1N1 influenza A viruses from swine in Ohio. *Vet. Microbiol.* **139**:132–139.
56. Yuan, L., K. Wen, M. S. Azevedo, A. M. Gonzalez, W. Zhang, and L. J. Saif. 2008. Virus-specific intestinal IFN-gamma producing T cell responses induced by human rotavirus infection and vaccines are correlated with protection against rotavirus diarrhea in gnotobiotic pigs. *Vaccine* **26**:3322–3331.